TELKOMNIKA, Vol.13, No.2, June 2015, pp. 401 ~ 412
ISSN: 1693-6930, accredited A by DIKTI, Decree No: 58/DIKTI/Kep/2013
DOI: 10.12928/TELKOMNIKA.v13i2.1467

Battery State of Charge Estimation with Extended Kalman Filter Using Third Order Thevenin Model

Low Wen Yao[1], Wirun A/l Prayun[2], J. A. Aziz*[3], Tole Sutikno[4]
[1,2,3]Department of Electrical Power Engineering, Faculty of Electrical Engineering,
Universiti Teknologi Malaysia, 81300 Skudai, Johor, Malaysia
4Department of Electrical Engineering, Faculty of Industrial Technology,
Universitas Ahmad Dahlan, Janturan, Umbulharjo 55164, Yogyakarta, Indonesia
*Corresponding author, e-mail: junaidi@fke.utm.my

Abstract

Lithium-ion battery has become the mainstream energy storage element of the electric vehicle. One of the challenges in electric vehicle development is the state-of-charge estimation of battery. Accurate estimation of state-of-charge is vital to indicate the remaining capacity of the battery and it will eventually maximize the battery performance and ensures the safe operation of the battery. This paper studied on the application of extended Kalman-filter and third order Thevenin equivalent circuit model in state-of-charge estimation of lithium ferro phosphate battery. Random test and pulse discharge test are conducted to obtain the accurate battery model. The simulation and experimental results are compared to validate the proposed state-of-charge estimation method.

Keywords: *Lithium Ion Battery, Battery Management System, State of Charge, Extended Kalman Filter, Energy Storage System*

1. Introduction

Over the years, depletion of non-renewable energy resources and the increment of fossil fuel price have encouraged the growing interests in renewable energy sources especially in transportation. Electric Vehicle (EV) is an example of the application of renewable energy sources in transportation. It is environmental friendly because it neither consumes the petrol nor produces the green house gaseous.

Lithium ion (Li-ion) battery has become the mainstream energy storage element in electric vehicle (EV). For instance, lithium manganate ($LiMn_2O_2$) battery has been used in Nissan Leaf EV, Chevrolet Volt and Renault Fluence whereas lithium ferro phosphate ($LiFePO_4$) battery has been used in BYD E6 [1]. Accurate state-of-charge (SoC) estimation is crucial to indicate the remaining capacity of the battery. The accurate information of SoC will eventually maximize battery performance and ensure the battery safe operation.

SoC is the indication of remaining battery capacity which is expressed in percentage. For instance, 100% refer to fully charged whereas 0% refer to fully discharged. Generally, SoC is defined as the ratio of the remaining charge of the battery and the total charge while the battery is fully charged at the same specific condition [1].

Several methods have been proposed in previous literature for SoC estimation [2]–[8]. Discharge test method [2] is one of the accurate approaches to calculate SoC. In this method, battery is discharged under specific temperature and current. The SoC is identified through discharge process. However, this method is only suitable for laboratory study and not suitable to be used for real time SoC estimation in electric vehicle.

Coulomb counting [3] is another popular approach for SoC estimation. In this method, SoC is calculated by accumulating charge/discharge current of battery. Application of this method enables real-time value of SoC to be calculated without the need of expensive devices. However, this method is highly dependent on the measured battery current which is disturbed measurement noise. The measurement drift would eventually influence the accuracy of this method. Moreover, initial SoC of battery is vital for this method while the initial value of SoC might not ready available in practical situation [1],[2].

Neural network model and fuzzy logic [4],[5] are also been applied for SoC estimation. In these methods, an input to output relationship is established by using neural network or fuzzy logic. Neither hypothesis nor prior knowledge of battery is required to be considered. However,

Received January 25, 2015; Revised March 11, 2015; Accepted March 27, 2015

a great training data are required to train the neural network and fuzzy logic. It also needs a lot of computation and powerful processing chips such as DSP. Moreover, the estimation error in the training data may influence the performance of these methods [1].

Kalman-filter [6]–[8] is also been used for SoC estimation. Kalman-filter is a recursive state estimator which estimates the state by using the information of the previous estimated state and the current measurement. Moreover, an optimal state estimation can be achieved by Kalman-filter because it has considered the process and measurement noises in the algorithm. Extended Kalman-filter (EKF) is the nonlinear version of Kalman-filter and it is suitable to be applied in the nonlinear system, such as battery. It is a very reliable method because it is not sensitive to the noises and it does not need the precise value of initial SoC. Besides from EKF, there are several version of Kalman-filter have been applied for SoC Estimation, such as sigma-point Kalman-filter [9], adaptive extended kalman filter [10], and adaptive sigma-point kalman filter [11]. However, compared to these algorithms, EKF has a lower complexity. Thus, a lower cost shall be expected for EKF SoC estimation system.

The accuracy of EKF SoC estimation is highly dependent on the accuracy of battery model. Thus, Thevenin equivalent circuit model provides good prediction on the runtime I-V characteristic of battery. Previous studies show that the accuracy of the predicted battery response is enhanced by applying higher order of Thevenin equivalent circuit model [12]. It is also proven that the third order Thevenin equivalent circuit model is reliable to capture the nonlinear dynamic characteristics of Li-ion battery [12],[13].

EKF SoC estimation, which is based on the first order [14] and the second order Thevenin equivalent circuit model [15] are presented in previous literatures. However, at present, there is no study applying the EKF SoC estimation on the third order Thevenin equivalent circuit model. Considering the fact that the third order Thevenin equivalent circuit model has better accuracy, in this paper, an EKF SoC estimation for lithium-ion battery is carried out based on the third order Thevenin equivalent circuit model. First, a third order Thevenin equivalent circuit model is developed based on the experimental data of battery tests. Then, the EKF algorithm is applied on the state-space equations of third order Thevenin equivalent circuit model to estimate the SoC. The method is then validated by comparing real SoC value to the estimated SoC value.

2. Battery Modeling

The third order Thevenin equivalent circuit model is illustrated in Figure 1. The battery model is formed by an open circuit voltage (OCV) source, a series resistance and three resistor-capacitor (RC) parallel networks in the series. The value of OCV is nonlinear and dependent on the SoC. The series resistance (R_S) represents the internal resistance of battery whereas the RC parallel networks (R_1, R_2, R_3, C_1, C_2, C_3) simulate the transient response of battery voltage. Based on Figure 1, the following equations can be obtained:

$$V_t = OCV - V_{RC1} - V_{RC2} - V_{RC3} - I_L R_S \tag{1}$$

$$\frac{dV_{RC1}}{dt} = \frac{I_L}{C_1} - \frac{V_{RC1}}{C_1 R_1} \tag{2}$$

$$\frac{dV_{RC2}}{dt} = \frac{I_L}{C_2} - \frac{V_{RC2}}{C_2 R_2} \tag{3}$$

$$\frac{dV_{RC3}}{dt} = \frac{I_L}{C_3} - \frac{V_{RC3}}{C_3 R_3} \tag{4}$$

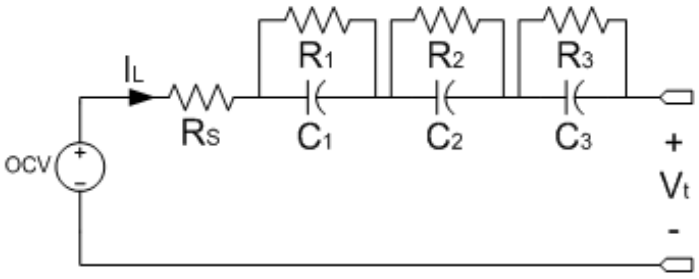

Figure 1. Third order Thevenin equivalent circuit model

In order to apply the battery model in EKF SoC estimation algorithm, the battery model is transformed as state-space equations. In this aspect, the SoC and the voltage drop across RC parallel networks are chosen as the state variable. SoC is expressed as Eq. (5), where SoC_0 is the initial SoC, C_N is the usable capacity (in the unit of Ah), and I_L is the battery current which has the negative value during charge and positive value when discharge. The overall state equation for third order Thevenin equivalent circuit model can be formulated as denoted in Eq. (6) and Eq. (7).

$$SoC = SoC_0 - \frac{100}{3600}\int_0^t \frac{I_L(t)}{C_N}dt \tag{5}$$

$$x = \begin{bmatrix} SoC & V_{RC1} & V_{RC2} & V_{RC3} \end{bmatrix}^T \tag{6}$$

$$\dot{x} = \begin{bmatrix} 0 & 0 & 0 & 0 \\ 0 & \frac{-1}{C_1R_1} & 0 & 0 \\ 0 & 0 & \frac{-1}{C_2R_2} & 0 \\ 0 & 0 & 0 & \frac{-1}{C_3R_3} \end{bmatrix} x + \begin{bmatrix} \frac{-100}{3600C_N} \\ \frac{1}{C_1} \\ \frac{1}{C_2} \\ \frac{1}{C_3} \end{bmatrix} I_L \tag{7}$$

Then, the state-space equation at time step k can be expressed as Eq. (8) and Eq. (9) by including the time interval Δt:

$$x_k = \begin{bmatrix} 1 & 0 & 0 & 0 \\ 0 & 1-\frac{\Delta t}{C_1R_1} & 0 & 0 \\ 0 & 0 & 1-\frac{\Delta t}{C_2R_2} & 0 \\ 0 & 0 & 0 & 1-\frac{\Delta t}{C_3R_3} \end{bmatrix} x_{k-1} + \begin{bmatrix} \frac{-100\Delta t}{3600C_N} \\ \frac{\Delta t}{C_1} \\ \frac{\Delta t}{C_2} \\ \frac{\Delta t}{C_3} \end{bmatrix} I_{L_{k-1}} \tag{8}$$

$$V_{t_k} = \begin{bmatrix} \frac{\partial OCV}{\partial SoC} & -1 & -1 & -1 \end{bmatrix} x_k + \begin{bmatrix} -R_S \end{bmatrix} \cdot I_{L_k} \tag{9}$$

3. Parameter Extraction of Battery Model

The parameterization of third order Thevenin equivalent circuit model is fairly straightforward. In this aspect, each parameters of battery model can be identified from the experimental data of battery test. In this paper, parameterization processes are arranged as follow:

(i) Battery tests.
(ii) Usable capacity.
(iii) OCV-SoC relationship.
(iv) Series resistance (R_S) and RC parallel networks parameters (R_1, R_2, R_3, C_1, C_2, C_3).

3.1. Battery Tests

The parameterization of battery starts with battery tests. The experimental set up for battery test is shown in Figure 2. In this paper, 3.2V, 18Ah lithium ferro phosphate battery is applied. An electronic load, IT8514C, with the rating of 120V, 240A, 1200W is used to discharge the battery. A data acquisition device, DAQ NI9219, from National Instrument is used to collect and store the measurement data into computer. NI9219 is capable of processing more than 100 samples per second with the accuracy of up to 5 decimal places. LabVIEW is used to store the battery data acquired from NI9219 DAQ. In this paper, the sampling rate is set to 6 samples per minute. Higher sampling rate is not preferable in this experiment because it requires a larger memory space.

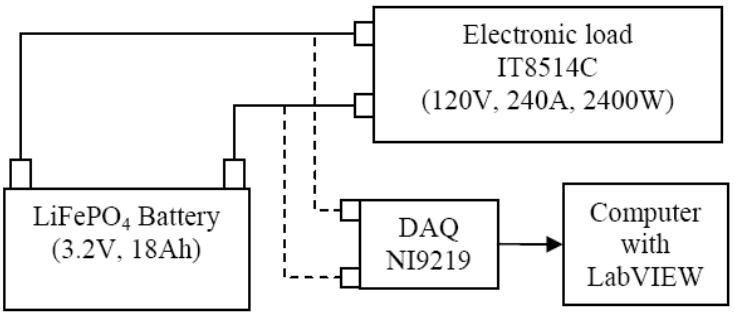

Figure 2. Experimental set up for battery test

In this paper, two battery tests are performed for battery modeling purpose. The first test is pulse discharge test. The test is made in order to identify the transient response and dynamic behavior of battery. Pulse discharge test consists of a sequence of constant discharge current and rest period as shown in Figure 3(a). The pulse discharged test is started with a fully charged battery. The battery is then discharged with a specific constant current to reduce 10% of the nominal capacity. Afterwards, a rest period is applied for the battery to achieve its equilibrium state before the next discharge. The discharge-rest cycle is repeated until battery voltage drops to 2 V. The current of 6A (0.333C), 9A (0.5C) and 18A (1C) are applied in pulse discharge test in order to find out the dynamic behavior of battery in different C-rate.

The second test is the random test in which the battery is randomly charged and discharged over a certain period of time as illustrated in Figure 3(b). This test is made in order to evaluate the accuracy of the developed third order battery model. In this test, battery is loaded with various currents, which include 3A (0.167C), 6A (0.333C), 9A (0.5C), 12A (0.667C), 18A (1C) and 36A (2C) of current. Moreover, some of the charging conditions are also included.

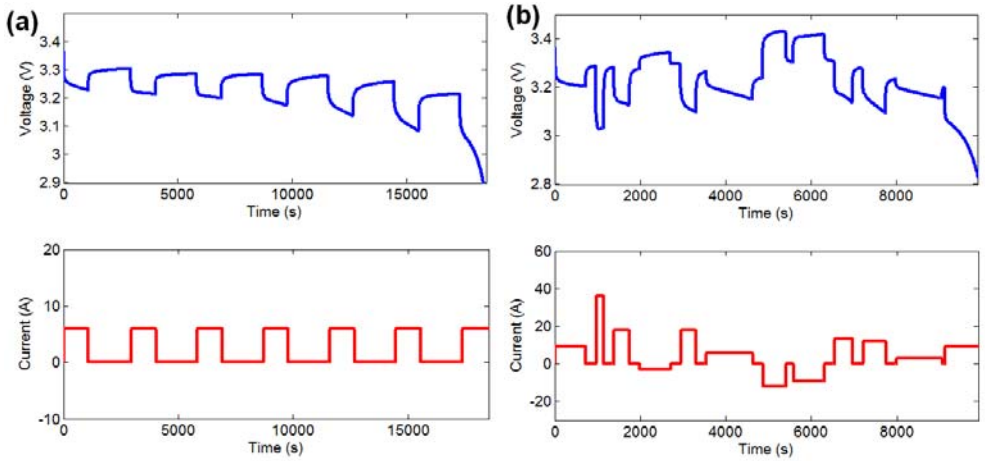

Figure 3. Voltage and current profiles for (a) pulse discharge test, and (b) random test

3.2. Usable Capacity

Usable capacity of battery varied according to charge/discharge current. It is not necessarily equal to the nominal capacity. In this aspect, the usable capacity is lower for high charge/discharge current. Based on the experimental result from battery test, the relationship between usable capacity and current is illustrated in Figure 4(a). The usable capacity of battery is expressed as Eq. (10).

$$C_N = 4.559 \cdot \exp\left[-0.4932 \cdot I_L\right] + 13.44 \cdot \exp\left[-0.0017 \cdot I_L\right] \quad (10)$$

3.3. OCV-SoC Relationship

Open circuit voltage is defined as the terminal voltage of battery at charge equilibrium condition. The value of OCV is directly dependent on the value of SoC. In this paper, OCV is identified from the pulse discharge test when the battery has rest. Several rest times are applied in pulse discharge test in determining OCV (i.e. 30 minutes for 0.33C, 60 minutes for 0.5C, and 45 minutes for 1C). The relationship between OCV and SoC is illustrated in Figure 4(b). As shown in the figure, lithium ferro phosphate battery has a flat OCV value within the SoC range of 40-90 %.

By using curve fitting, a fifth-order polynomial equation can be formulated to represent the OCV-SoC relationship as denoted in Eq. (11). The parameters in Eq. (11) are tabulated in Table 1.

$$OCV = a_1 SoC^5 + a_2 SoC^4 + a_3 SoC^3 + a_4 SoC^2 + a_5 SoC + a_6 \quad (11)$$

Table 1. Parameters of Eq. (11)

Parameter	Value
a_1	4.513×10^{-10}
a_2	-1.295×10^{-7}
a_3	1.505×10^{-5}
a_4	-8.927×10^{-4}
a_5	2.764×10^{-2}
a_6	2.918

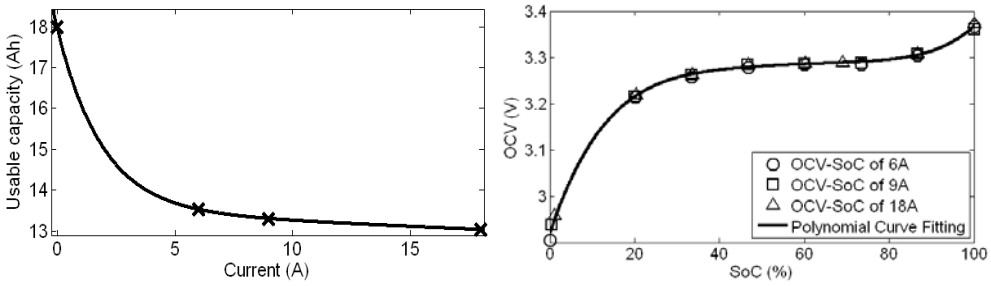

Figure 4. Ralationship between (a) usable capacity and current, and (b) open circuit voltage and state-of-charge

3.4. Series Resistance and RC Parallel Networks Parameters

The transient voltage response for discharge and rest are illustrated in Figure 5. The series resistance and RC parallel networks parameters can be identified from the transient voltage response during the rest period [16]. The voltage across RC parallel networks for loaded and rest conditions are denoted as Eq. (12), where i = 1, 2, 3, t_0 is the beginning time, t_d is the discharge ending time and t_r is the rest ending time of the period.

$$V_{RC_i} = I_L \cdot R_i \cdot \left[1 - \exp\left(\frac{-(t-t_0)}{R_i C_i}\right)\right], \quad t_0 < t < t_d, \quad I_L \neq 0$$
$$V_{RC_i} = V_{RC_i}(t_d) \cdot \left[\exp\left(\frac{-(t-t_d)}{R_i C_i}\right)\right], \quad t_d < t < t_r, \quad I_L = 0 \tag{12}$$

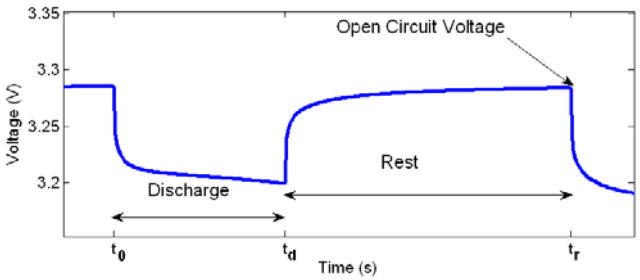

Figure 5. Transient voltage response for pulse discharge test

By applying MATLAB curve fitting tool, transient voltage response for rest period can be represented by Eq. (13).

$$V_t = OCV - b_S - b_1 \cdot \exp[-c_1 \cdot (t - t_d)] - b_2 \cdot \exp[-c_2 \cdot (t - t_d)] - b_3 \cdot \exp[-c_3 \cdot (t - t_d)] \tag{13}$$

Afterwards, the parameters for third order Thevenin equivalent circuit model can be identified as denoted in Eqs. (14)-(16), where i = 1, 2, and 3.

$$R_i = \frac{b_i}{I_L \cdot (1 - \exp[-c_i \cdot (t_d - t_0)])} \tag{14}$$

$$C_i = \frac{1}{c_i \cdot R_i} \tag{15}$$

$$R_S = \frac{b_S}{I_L} \tag{16}$$

Based on the results from curve fitting method, the series resistance and RC parallel networks parameters can be identified as tabulated in Table 2. The validation of battery model is made by comparing experimental and simulation results of random test as shown in Figure 6. It can be seen that a significant diverge exist when SoC is below 20 %. However, since electric vehicle is usually operated within 30 % to 100 % SoC [17], the accuracy of model is still considered acceptable. The comparative analysis shows that the root-mean-square (RMS) of modeling errors is 32.265 mV. Based on the good match between experiment and simulation results, the developed model is validated.

Table 2. Parameters for Third order Thevenin Equivalent Circuit Model

Parameters	Value
R_1	0.006 Ω
R_2	0.003 Ω
R_3	0.002 Ω
C_1	2127.949 F
C_2	37348.281 F
C_3	286996.625 F
R_S	0.003 Ω

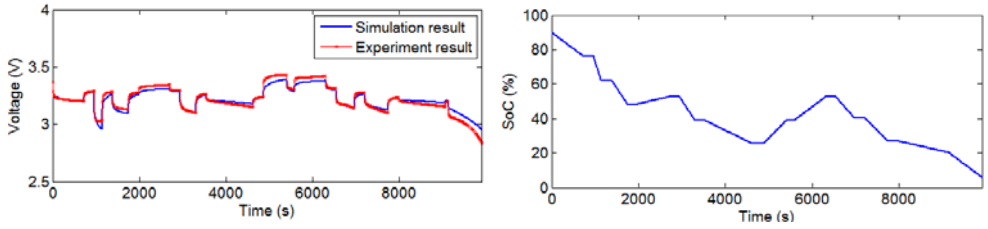

Figure 6. Experimental and simulation results of random test

4. Extended Kalman-Filter for State-of-Charge Estimation

State-space model for battery as expressed in Eqs. (8) and (9) are utilized to estimate the SoC. The typical state-space representation for a nonlinear system is expressed as Eq. (17), where k is the time index, x_k is the nonlinear state, u_k is the control input, y_k is the system output, w_k is a discrete time process white noise with covariance matrix Q, and v_k is a discrete time measurement white noise with covariance matrix R.

$$\begin{aligned} x_{k+1} &= f(x_k, u_k) + w_k \\ y_k &= g(x_k, u_k) + v_k \\ w_k &\sim (0, Q), v_k \sim (0, R) \end{aligned} \tag{17}$$

In this application, nonlinear state is defined as Eq. (6), control input is defined as battery current, and system output is defined as battery terminal voltage. By applying Jacobian matrix of partial derivatives of function f and g with respect to x_{k-1} and u_{k-1}, state-space equations are transformed as Eq. (18).

$$\begin{aligned} x_{k+1} &= A_k x_k + B_k u_k + w_k \\ y_k &= C_k x_k + D_k u_k + v_k \end{aligned} \tag{18}$$

where,

$$A_k = \frac{\partial f(x_k,u_k)}{\partial x_k}, \quad B_k = \frac{\partial f(x_k,u_k)}{\partial u_k}, \\ C_k = \frac{\partial g(x_k,u_k)}{\partial x_k}, \quad D_k = \frac{\partial g(x_k,u_k)}{\partial u_k} \tag{19}$$

As denoted in Eq. (8) and Eq. (9), the matrix A_k, B_k, C_k, D_k are expressed in Eqs. (20)-(23) respectively.

$$A_k = \begin{bmatrix} 1 & 0 & 0 & 0 \\ 0 & 1-\frac{\Delta t}{C_1R_1} & 0 & 0 \\ 0 & 0 & 1-\frac{\Delta t}{C_2R_2} & 0 \\ 0 & 0 & 0 & 1-\frac{\Delta t}{C_3R_3} \end{bmatrix} \tag{20}$$

$$B_k = \begin{bmatrix} \frac{-100\cdot\Delta t}{3600\cdot C_N} & \frac{\Delta t}{C_1} & \frac{\Delta t}{C_2} & \frac{\Delta t}{C_3} \end{bmatrix}^T \tag{21}$$

$$C_k = \begin{bmatrix} \frac{\partial OCV}{\partial SoC} & -1 & -1 & -1 \end{bmatrix} \tag{22}$$

$$D_k = \begin{bmatrix} -R_s \end{bmatrix} \tag{23}$$

The initialization of EKF algorithm is given by Eq. (24), where P_0^+ is the prediction error covariance matrix.

$$k = 0, \\ \hat{x}_0^+ = E[x_0], \\ P_0^+ = E\left[(x_0 - \hat{x}_0^+)\cdot(x_0 - \hat{x}_0^+)^T\right] \tag{24}$$

The computation of EKF algorithm consists of five steps. The variable which computed before system measurement (*priori*) is denoted by superscript "–" whereas variable which computed after system measurement (*posteriori*) is denoted by superscript "+".

(i) State estimation time update:

$$\hat{x}_k^- = A_{k-1}\hat{x}_{k-1}^+ + B_{k-1}u_{k-1} \tag{25}$$

where $\hat{x}_k^-$ is priori state estimate at step *k* given the process prior to step *k*, whereas $\hat{x}_{k-1}^+$ is the posteriori state estimate at step *k–1*.

(ii) Error covariance time update:

$$P_k^- = A_{k-1}P_{k-1}^+A_{k-1}^{\mathrm{T}} + Q \tag{26}$$

where P_k^- is the priori error covariance at step *k* whereas is P_{k-1}^+ the posteriori error covariance at step *k–1*.

(iii) Calculation of Kalman gain:

$$K_k = P_k^-C_k^T\left[C_kP_k^-C_k^T + R\right]^{-1} \tag{27}$$

(iv) State estimate measurement update:

$$\hat{x}_k^+ = \hat{x}_k^- + K_k\left(y_k - C_k\hat{x}_k^- - D_k u_k\right) \tag{28}$$

In this stage, posteriori state is estimated. y_k is the measurement output. In this case, y_k is the real-time terminal voltage of battery.

(v) Error covariance measurement update:

$$P_k^+ = \left(I - K_k C_k\right)P_k^- \tag{29}$$

In this stage, posteriori error covariance is estimated. The computing step is then repeated again from (i) to (v).

5. Result and Validation

In this section, the state-space equations for third order Thevenin equivalent circuit model are employed for SoC estimation. The validation of EKF SoC estimation is done by comparing experimental SoC and the estimated SoC. In this aspect, the experimental SoC is measured by using discharge test method. Eq. (5) is used in discharge test method with the pre-known value of SoC.

5.1. Selection of Initial Condition and Noise Covariances

The initial state (x_0), error covariance (P_0), process noise covariance (Q) and sensor noise covariance (R) are chosen as denoted in Eqs. (30)-(33). The initial SoC for EKF algorithm is set to 60%.

$$x_0 = \begin{bmatrix} 60 & 0 & 0 & 0 \end{bmatrix}^T \tag{30}$$

$$P_0 = \begin{bmatrix} 2500 & 0 & 0 & 0 \\ 0 & 0.0001 & 0 & 0 \\ 0 & 0 & 0.0001 & 0 \\ 0 & 0 & 0 & 0.0001 \end{bmatrix} \tag{31}$$

$$Q = \begin{bmatrix} 0.0001 & 0 & 0 & 0 \\ 0 & 0.0001 & 0 & 0 \\ 0 & 0 & 0.0001 & 0 \\ 0 & 0 & 0 & 0.0001 \end{bmatrix} \tag{32}$$

$$R = \begin{bmatrix} 0.004 \end{bmatrix} \tag{33}$$

5.2. Validation of EKF State-of-Charge Estimation

Random test is used to evaluate the performance of EKF SoC estimation. The experimental SoC for random test is compared to estimated SoC illustrated in Figure 7(a). As illustrated in Figure 7(a), although the initial SoC for EKF algorithm has deviate significantly to the real SoC, EKF is still able to estimate the accurate value of SoC within a short time. In this aspect, the root-mean-square (RMS) SoC estimation error is 3.5934 %. Moreover, the model output from EKF estimation is also well matched with the measured value of battery voltage as shown in Figure 8(a).

The EKF SoC estimation technique is further validated with pulse discharge tests. The experimental SoC and EKF estimated SoC for pulse discharge tests of 0.33C, 0.5C and 1C are shown in Figure 7(b), Figure 7(c), and Figure 7(d) respectively. The RMS error for SoC estimation is tabulated in Table 3. The comparative analysis shows the good match between

experiment and estimated SoC for pulse discharge test with RMS error of less than 2%. Moreover, the model outputs for EKF estimation are also well matched with the measured value of battery voltage for pulse discharge tests of 0.33C, 0.5C and 1C as shown in Figure 8(b), Figure 8(c), and Figure 8(d) respectively.

Table 3. RMS SoC Estimation error for Pulse Discharge Tests

Current (C)	RMS error for SoC Estimation (%)
0.33	1.417
0.5	1.881
1	1.611

Based on the good match between experiment and EKF estimated SoC, the performance of the developed SoC estimation method is validated.

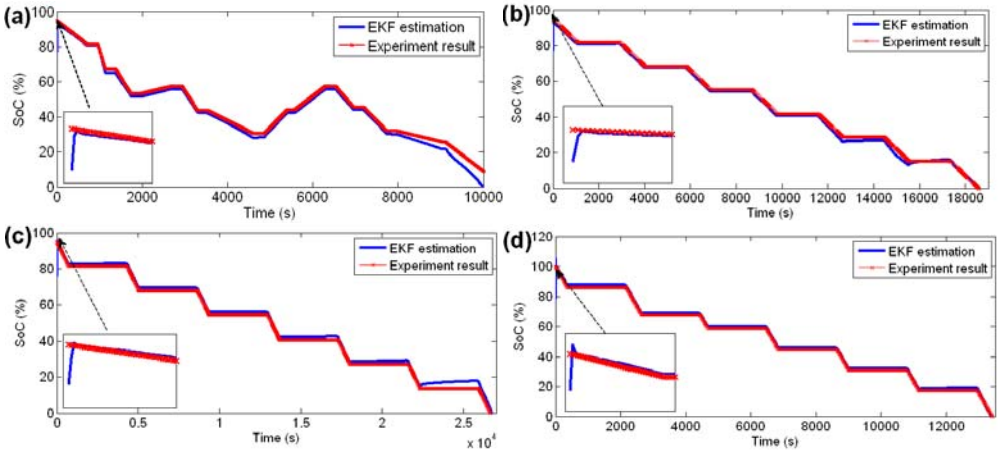

Figure 7. Comparison between experimental SoC and EKF estimated SoC for (a) random test, (b) 0.33C pulse discharge test, (c) 0.5C pulse discharge test, and (d) 1C pulse discharge test

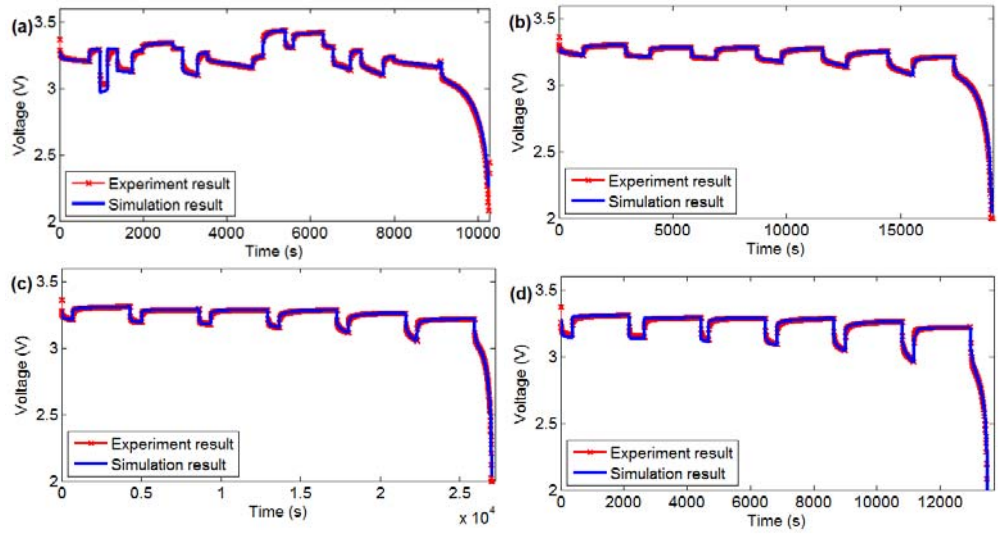

Figure 8. Comparison between experimental and simulation voltages for (a) random test, (b) 0.33C pulse discharge test, (c) 0.5C pulse discharge test, and (d) 1C pulse discharge test

5.3. EKF State-of-Charge Estimation using Second Order Thevenin Model

In order to compare the performance of the proposed SoC estimation method, a study of EKF SoC estimation using second order Thevenin equivalent circuit model. The parameters for the second order Thevenin model are tabulated in Table 4.

Table 4. Parameters for Second order Thevenin Equivalent Circuit Model

Parameters	Value
R_1	0.0045 Ω
R_2	0.0045 Ω
C_1	10000 F
C_2	150000 F
R_S	0.005 Ω

Random test and pulse discharged tests are used to evaluate the performance the SoC estimation. As illustrated in Figure 9, by using second order Thevenin model in EKF algorithm, the SoC estimation can still perform well. In this aspect, the estimated SoC is well match with the experiment result. However, as illustrated in the Figure, a bigger deviation is found if the second order Thevenin model is applied. The RMS error of the battery tests are also been tabulated in Table 5. The error analysis shows that EKF SoC estimation with second order Thevenin model gives a larger error. This is because the performance of EKF algorithm is highly dependent on the accuracy of the battery model. The propose SoC estimation method gives a better and reliable result because the third order Thevenin model is more accurate than the second order Thevenin model.

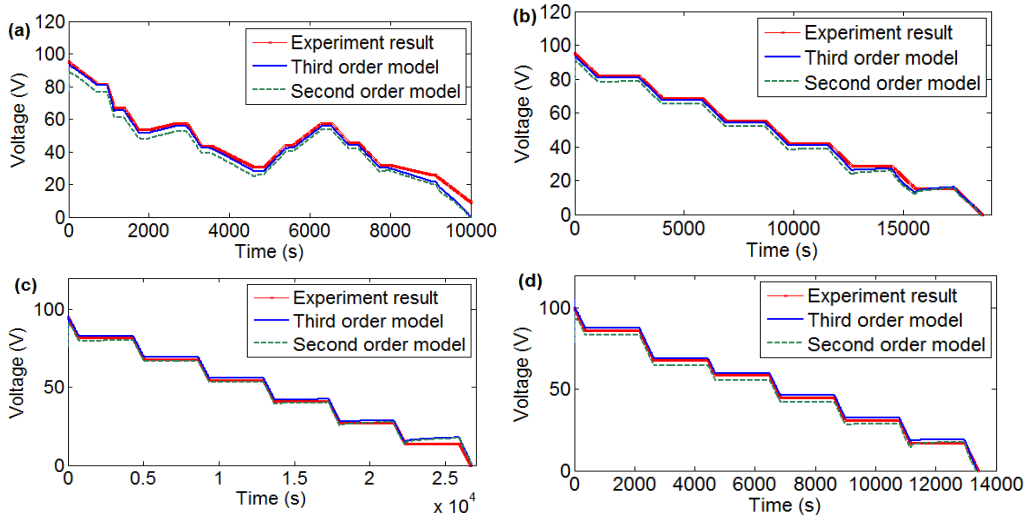

Figure 9. Comparison between experimental SoC and EKF estimated SoC with second and third order Thevenin model for (a) random test, (b) 0.33C pulse discharge test, (c) 0.5C pulse discharge test, and (d) 1C pulse discharge test

Table 5. RMS SoC Estimation error for EKF SoC Estimation using Second Order Thevenin Model

Battery tests	RMS error for SoC Estimation (%)
Random test	5.047
0.33 C Pulse Discharge Test	2.794
0.5 C Pulse Discharge Test	1.642
1 C Pulse Discharge Test	3.250

6. Conclusion

In this paper, an EKF SoC estimation technique has been developed based on the state space equation of third order Thevenin equivalent circuit model. It can be concluded that the proposed EKF technique is able to produce an accurate estimation of the SoC with RMS error of less than 3.6%. Compared to EKF SoC estimation with second order Thevenin equivalent circuit model, the developed SoC estimation technique provides an improved accuracy with a lesser RMS error. This is due to the high accuracy of the third order Thevenin equivalent circuit model. Moreover, even the initial SoC value is an unknown, the EKF algorithm could estimate the SoC with a good accuracy. Hence, by using an accurate third order Thevenin model, EKF could be a reliable algorithm for SoC estimation.

Acknowledgements

The authors gratefully acknowledge the financial support of Zamalah Scholarship, Research University Grant (Vot No. : 00G46) and Exploratory research Grant Scheme (Vot No. : RJ130000.7823.4L126) which provided by Ministry of Higher Education Malaysia and Universiti Teknologi Malaysia.

References

[1] Lu L, Han X, Li J, Hua J, Ouyang M. A review on the key issues for lithium-ion battery management in electric vehicles*. J Power Sources*. 2013; 226: 272–88.
[2] Piller S, Perrin M, Jossen A. Methods for state-of-charge determination and their applications. *J Power Sources*. 2001; 96(1): 113–20.
[3] Ng KS, Moo C-S, Chen YP, Hsieh YC. Enhanced coulomb counting method for estimating state-of-charge and state-of-health of lithium-ion batteries. *Applied Energy*. 2009; 86(9): 1506–11.
[4] Cheng HC, Dong D, Zhi YL, Hua Z. *Artificial neural network in estimation of battery state of-charge (SOC) with nonconventional input variables selected by correlation analysis.* Proceedings International Conference on Machine Learning and Cybernetics. Beijing. 2002: 1619–25.
[5] Cai CH, Du D, Liu ZY. *Battery state-of-charge (SOC) estimation using adaptive neuro-fuzzy inference system (ANFIS).* The 12th IEEE International Conference on Fuzzy Systems. St. Louis. 2003: 1068–73.
[6] Plett GL. Extended Kalman filtering for battery management systems of LiPB-based HEV battery packs*. J Power Sources*. 2004; 134(2): 252–61.
[7] Plett GL. Extended Kalman filtering for battery management systems of LiPB-based HEV battery packs*. J Power Sources*. 2004; 134(2) :262–76.
[8] Plett GL. Extended Kalman filtering for battery management systems of LiPB-based HEV battery packs*. J Power Sources*. 2004; 134(2): 277–92.
[9] He W, Williard N, Chen C, Pecht M. State of charge estimation for electric vehicle batteries using unscented kalman filtering. *Microelectron Reliab*. 2013; 53(6): 840–7.
[10] He H, Xiong R, Zhang X, Sun F, Fan J, Member S. State-of-Charge Estimation of the Lithium-Ion Battery Using an Adaptive Extended Kalman Filter Based on an Improved Thevenin Model. *IEEE Trans Veh Technol*. 2011; 60(4): 1461–9.
[11] Sun F, Hu X, Zou Y, Li S. Adaptive unscented Kalman filtering for state of charge estimation of a lithium-ion battery for electric vehicles. *Energy*. 2011; 36(5): 3531–40.
[12] Kroeze RC, Krein PT. *Electrical battery model for use in dynamic electric vehicle simulations*. 2008 IEEE Power Electron Spec Conf. Rhodes. 2008: 1336–42.
[13] Hentunen A, Lehmuspelto T, Suomela J. *Electrical battery model for dynamic simulations of hybrid electric vehicles*. 2011 IEEE Vehicle Power and Propulsion Conference. Chicago. 2011: 1–6.
[14] Lee S, Kim J, Lee J, Cho BH. State-of-charge and capacity estimation of lithium-ion battery using a new open-circuit voltage versus state-of-charge. *J Power Sources*. 2008; 185(2): 1367–73.
[15] Windarko NA, Choi J-H. LiPB Battery SOC Estimation Using Extended Kalman Filter Improved with Variation of Single Dominant Parameter. *J Power Electron*. 2012; 12(1): 40–48.
[16] Lam L, Bauer P, Kelder E. *A practical circuit-based model for Li-ion battery cells in electric vehicle applications*. 2011 IEEE 33rd International Telecommunications Energy Conference (INTELEC). Amsterdam. 2011: 1–9.
[17] Chen Z, Fu Y, Mi CC. State of Charge Estimation of Lithium-Ion Batteries in Electric Drive Vehicles Using Extended Kalman Filtering*. IEEE Trans Veh Technol*. 2013; 62(3): 1020–30.